HST Kernel-Phase Interferometry: Binary Demographics of Brown Dwarfs from Birth to Maturity

Samuel M. Factor, Adam L. Kraus
Dept. of Astronomy, The Univ. of Texas at Austin

The University of Texas at Austin
Department of Astronomy
College of Natural Sciences

Contact Information
Email: sfactor@utexas.edu
Website: smfactor.github.io

S. Factor is P.I. of HST cycle 24 & 29 archival projects 14561 & 16612 which support this work.

Kernel phases are self-calibrating observables **used for high-contrast imaging at or even below λ/D. We** have used this technique and **searched for companions to young and old brown dwarfs** in the *HST*/ACS and *HST*/NICMOS archives, respectively. We preliminarily detected 6 new candidate companions. We then modeled the binary demographics **and find both populations favor tight separation and equal mass companions.** Comparing the two populations, we note a significant excess of young wide companions over the field. **We conclude that dynamical evolution dissolves the widest systems and wide companions only survive if they are born in low density regions.** GMT will have ~10x higher resolution than HST, enabling us to definitively resolve the peak of the semimajor axis distribution.

What is a Kernel-Phase?

Non-redundant aperture masking interferometry (NRM/AMI) uses a pupil-plane mask which blocks ~95% of gathered light, imposing a *severe* flux limit. **Kernel-phase interferometry (KPI) models the *full aperture* as a grid of sub-apertures** (Fig. 1). Kernel phases, an abstraction of closure phases used with NRM/AMI (Martinache 2010), are calculated from linear combinations of the Fourier phase (sampled according to the aperture model) and can be used to infer the source geometry.

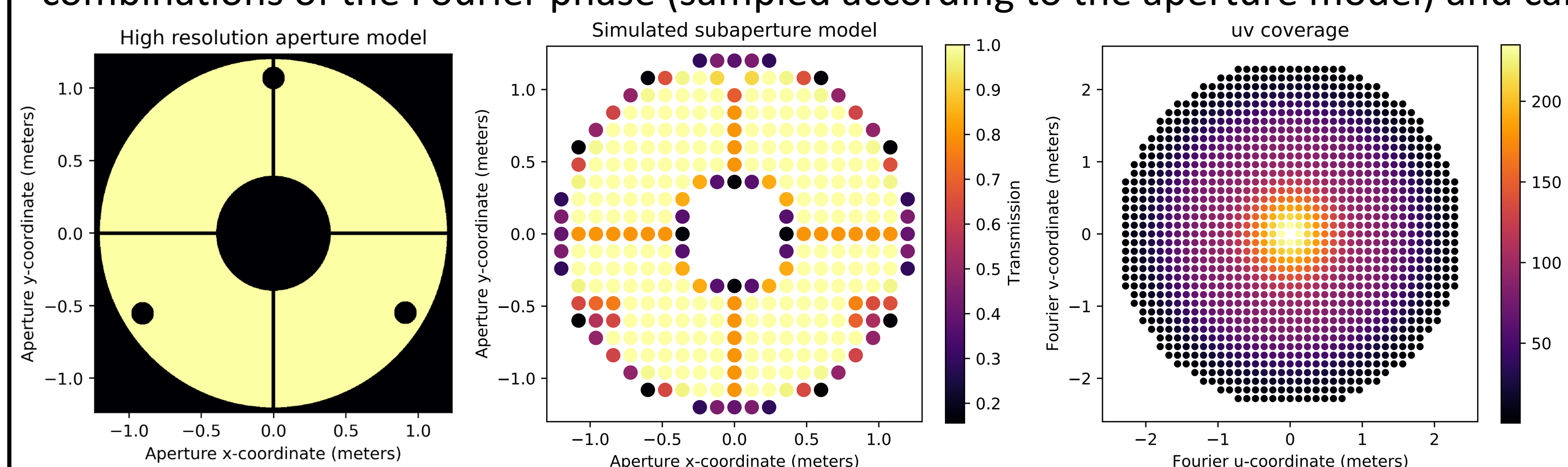

Figure 1: *Left*: HST aperture as seen by ACS. The NICMOS pupil is rotated 45° and includes cold masks. *Center*: ACS aperture model with 315 simulated sub-apertures, colored by their transparency. The model used with NICMOS is lower resolution. *Right*: The corresponding 622 distinct baselines, colored by their redundancy. This model generates 308 kernel-phases.

The kernel-phase transfer matrix is calculated using singular value decomposition and corresponds to linear combinations which self calibrate out (to first order) phase errors across the pupil, producing phase-like observables which only depend on the source geometry. **This technique can achieve similar detection limits to NRM in a fraction of the time and can be applied to dimmer sources, where NRM is not feasible, as well as to archival data sets.**

Binary Search

Old/Field (NICMOS) | Young/Tau & USco (ACS)

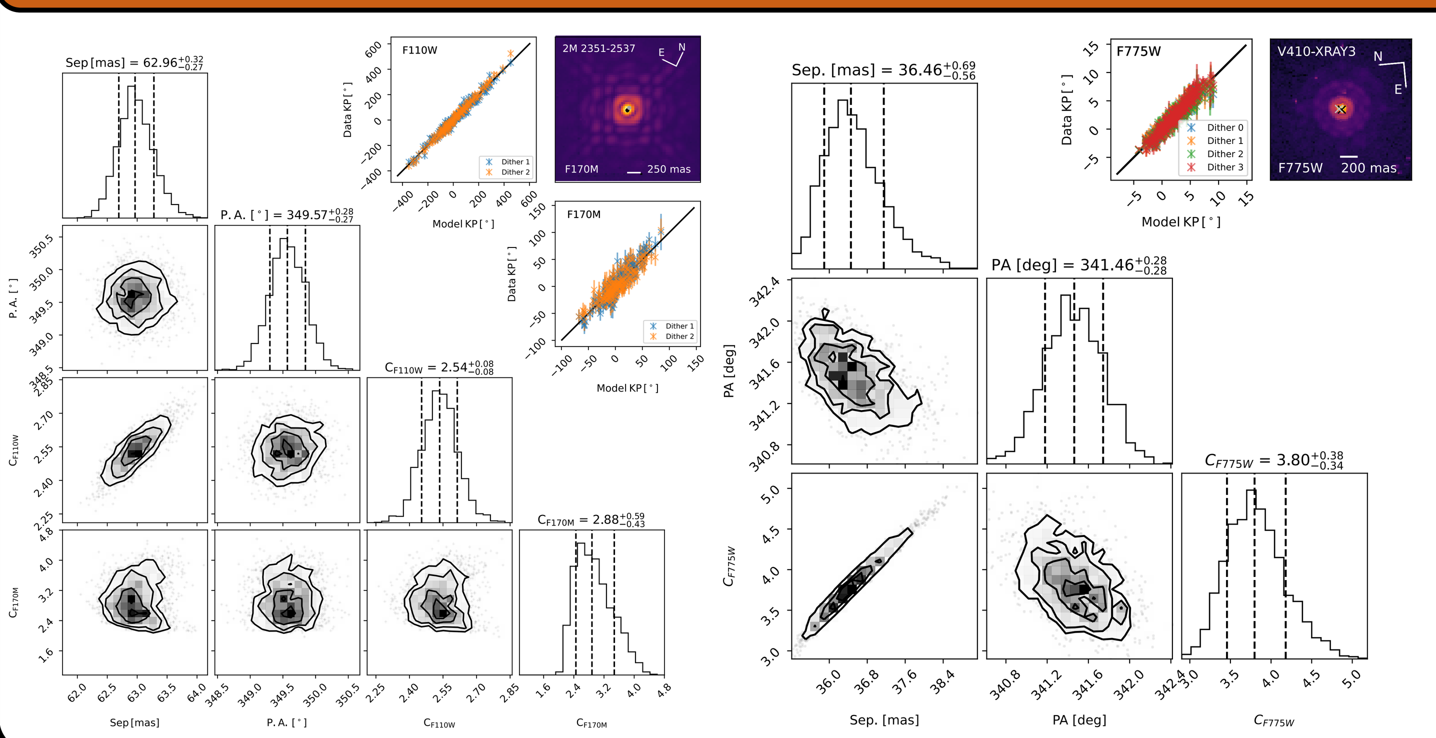

Figure 2: Example compact BD binary detections ($\lesssim 0.5\,\lambda/D$) in the NICMOS field age sample (*left*) and the ACS/HRC young sample (*right*). *Lower Left*: Corner plots showing the posteriors of the fits with median and ±1σ values. *Top Right*: Data kernel phases plotted against the best-fit model kernel phases for each filter and/or dither position.

We have analyzed two datasets to search for compact binary systems: 1) The entire NICMOS1 imaging archive of field-age brown dwarfs (in F110W and F170M) and 2) ACS/HRC observations of young very-low-mass objects in Taurus and Upper Scorpius. This is the first application of KPI to visible wavelength observations. **We fit the data using a Bayesian routine** (`PyMultiNest`; Buchner et al. 2014) **and calculate detection limits using a similar method to NRM**. New realizations of the noise are created by scrambling the model subtracted kernel-phases. We then fit the contrast on a grid in separation and PA and the 99% confidence contrast is the contrast at which 99% of all fits are fainter. Fig. 2 shows example binary detections from the two samples and the upper right panels of Fig. 3 show the detections and sensitivity of our surveys.

Population Analysis

Old/Field (NICMOS) | Young/Tau & USco (ACS)

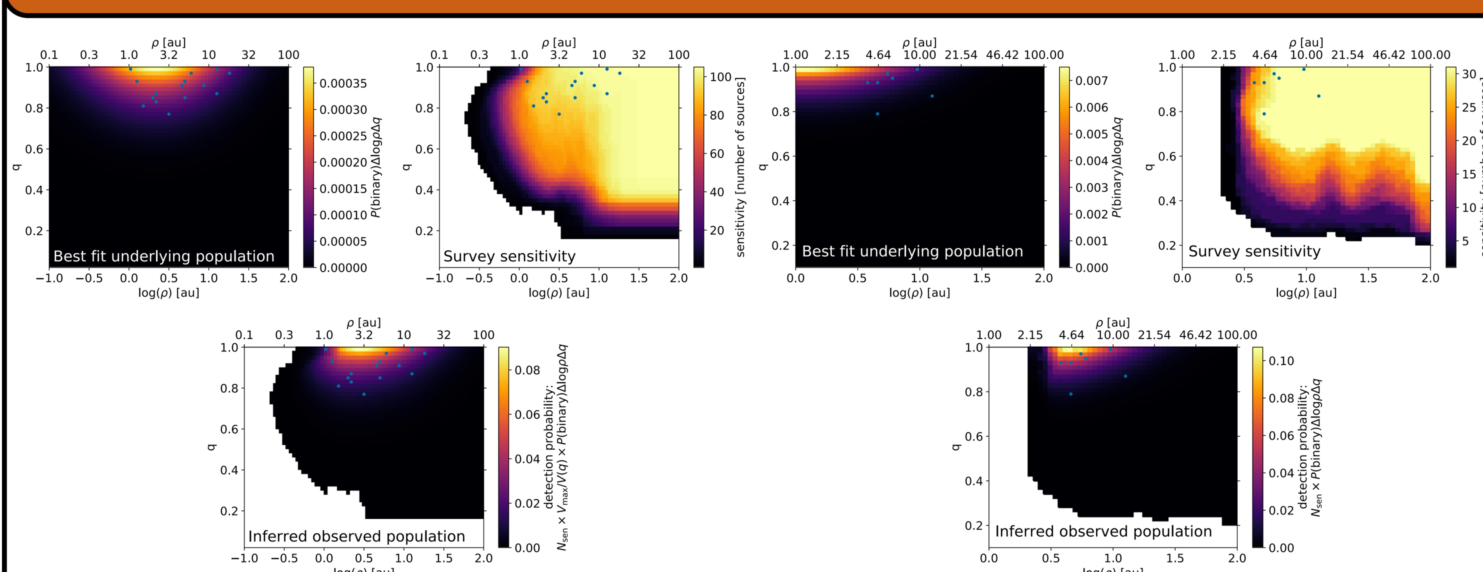

Figure 3: Progression from underlying population and sensitivity to observed population for our two surveys. Blue points are detected companions. The observed population (the probability that a companion could be detected in a bin, *bottom center*) is calculated by applying our sensitivity (in number of targets, *top right*) to the inferred population (*top left*). We also account for Malmquist bias in the field sample.

We model our detections with a companion frequency F, mass-ratio (q) power-law index γ, and log-normal projected-separation mean $\overline{\log(\rho)}$ and $\sigma_{\log(\rho)}$. We convert contrast to mass ratios using ATMO 2020 and DUSTY models (Phillips et al. 2020, Chabrier et al. 2000, Baraffe et al. 2002).

Old/Field (NICMOS)

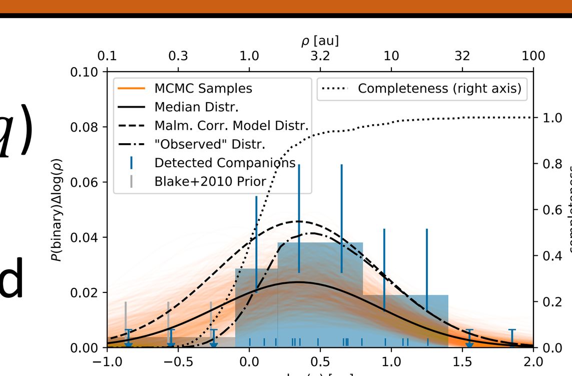

Figure 4: 1D detections and model population for the field sample showing the importance of constraining the unresolved ($\rho < 1$ au) companion frequency to $2.5^{+8.6}_{-2.6}\%$ using an RV survey based prior (Blake et al. 2010). Without this, the inferred mean separation is unphysically tight ($\overline{\rho} \sim R_{\rm Jup}$).

Conclusions

Old/Field (NICMOS)

Figure 5: Field-age binary demographics as a function of primary mass, putting our results in context. Results from this work are shown on a color scale for different assumed field ages, which only affects the derived masses and therefore γ.

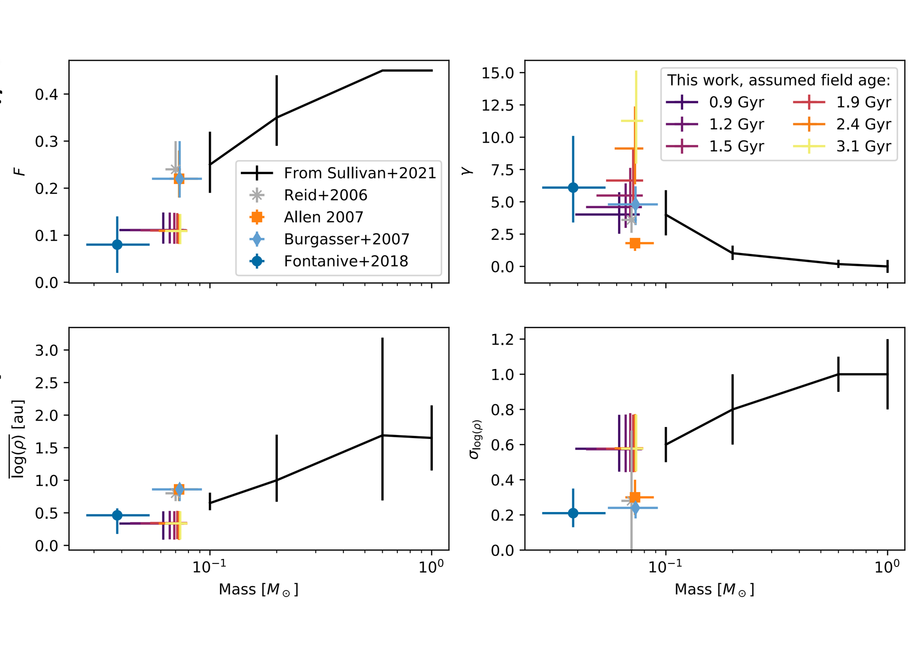

1) We find a companion distribution centered at a tighter separation than previous studies (due to our higher angular resolution) **that strongly favors equal mass systems** (q~1). Fig. 5 compares our field population to literature values.
2) We find an excess of *young* wide separation companions compared to the old/field population (see Fig. 6). Thus, dynamical evolution *in the birth cluster* significantly sculpts the wide binary population (interactions in the field are not strong enough to remove companions). **3) Wide separation ($\rho > 10$ au) systems only survive if they are born in low density star forming regions** (i.e. most wide systems born in high density regions are dissolved). Our field population of wide separation companions is consistent with our young population diluted with single systems by 90%, the fraction of stars born in massive star forming regions.

Young/Tau & USco vs. Old/Field

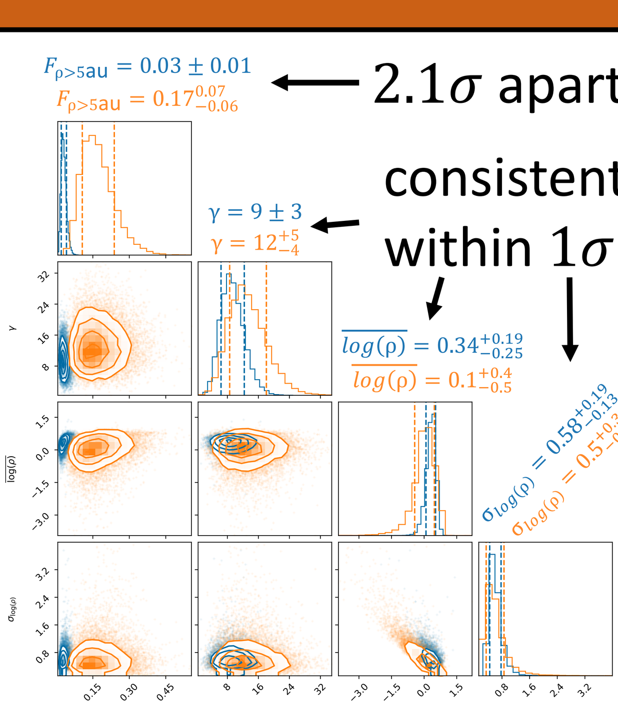

Figure 6: Corner plot showing the 1- and 2D posteriors of our demographic fits comparing the young (orange) and old/field age (blue) populations. We choose to compare $F_{\rho>5\rm au}$ where the ACS (young) survey is 90% complete.